

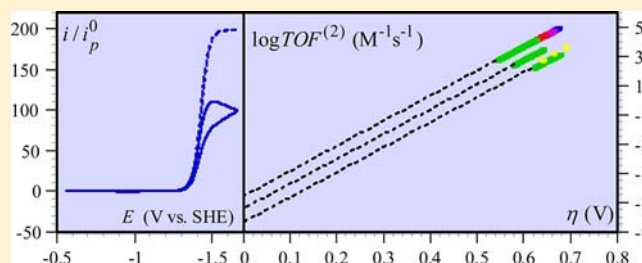
# Turnover Numbers, Turnover Frequencies, and Overpotential in Molecular Catalysis of Electrochemical Reactions. Cyclic Voltammetry and Preparative-Scale Electrolysis

Cyrille Costentin, Samuel Drouet, Marc Robert, and Jean-Michel Savéant\*

Laboratoire d'Electrochimie Moléculaire, Unité Mixte de Recherche Université–CNRS No. 7591, Université Paris Diderot, Sorbonne Paris Cité, Bâtiment Lavoisier, 15 rue Jean de Baïf, 75205 Paris Cedex 13, France

**S** Supporting Information

**ABSTRACT:** The search for efficient catalysts to face modern energy challenges requires evaluation and comparison through reliable methods. Catalytic current efficiencies may be the combination of many factors besides the intrinsic chemical properties of the catalyst. Defining turnover number and turnover frequency (TOF) as reflecting these intrinsic chemical properties, it is shown that catalysts are not characterized by their TOF and their overpotential ( $\eta$ ) as separate parameters but rather that the parameters are linked together by a definite relationship. The  $\log \text{TOF}-\eta$  relationship can often be linearized, giving rise to a Tafel law, which allows the characterization of the catalyst by the value of the TOF at zero overpotential ( $\text{TOF}_0$ ). Foot-of-the-wave analysis of the cyclic voltammetric catalytic responses allows the determination of the TOF,  $\log \text{TOF}-\eta$  relationship, and  $\text{TOF}_0$ , regardless of the side-phenomena that interfere at high current densities, preventing the expected catalytic current plateau from being reached. Strategies for optimized preparative-scale electrolyses may then be devised on these bases. The validity of this methodology is established on theoretical grounds and checked experimentally with examples taken from the catalytic reduction of  $\text{CO}_2$  by iron(0) porphyrins.



The search for efficient catalysts to face modern energy challenges requires evaluation and comparison through reliable methods. Catalytic current efficiencies may be the combination of many factors besides the intrinsic chemical properties of the catalyst. Defining turnover number and turnover frequency (TOF) as reflecting these intrinsic chemical properties, it is shown that catalysts are not characterized by their TOF and their overpotential ( $\eta$ ) as separate parameters but rather that the parameters are linked together by a definite relationship. The  $\log \text{TOF}-\eta$  relationship can often be linearized, giving rise to a Tafel law, which allows the characterization of the catalyst by the value of the TOF at zero overpotential ( $\text{TOF}_0$ ). Foot-of-the-wave analysis of the cyclic voltammetric catalytic responses allows the determination of the TOF,  $\log \text{TOF}-\eta$  relationship, and  $\text{TOF}_0$ , regardless of the side-phenomena that interfere at high current densities, preventing the expected catalytic current plateau from being reached. Strategies for optimized preparative-scale electrolyses may then be devised on these bases. The validity of this methodology is established on theoretical grounds and checked experimentally with examples taken from the catalytic reduction of  $\text{CO}_2$  by iron(0) porphyrins.

## INTRODUCTION

Modern energy challenges involve the catalytic activation toward reduction and/or oxidation of inert molecules such as water, dioxygen, and carbon dioxide.<sup>1–10</sup> A huge number of possible catalysts, notably from transition metal coordination chemistry, are available or can be made available for this purpose by searching to minimize the overpotential and maximize the catalytic efficiency. Systematic investigation of this discouragingly large number of possibilities under conditions of real preparative-scale electrolysis seems too much of a formidable task, the more so in that overpotential and catalytic efficiency are both combinations of intrinsic chemical characteristics of the catalyst, transport factors, cell geometry, and a variety of additional parameters. It would therefore be helpful to find a non-destructive method<sup>11</sup> allowing a quick determination of the essential reactivity parameters of the catalyst, regardless of side factors, its intrinsic turnover number (TON) and its turnover frequency (TOF). We propose for this purpose a foot-of-the-wave analysis applicable to standard cyclic voltammograms, leading to the determination of these parameters for both heterogeneous and homogeneous catalytic reactions. The following discussion is restricted to molecular catalysis where the catalytic species is a well-defined molecule with a well-defined standard potential, as opposed to “electrocatalytic” reactions where the catalysts are not clearly identified “surface states”.

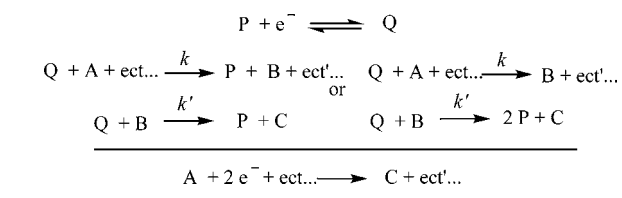
Establishing the applicability and reliability of this approach will involve considering three types of commonly encountered side-phenomena, namely consumption of the substrate, deactivation of the catalyst, and inhibition by products. It will be shown on theoretical grounds how the foot-of-the-wave strategy applied to cyclic voltammograms allows one to get rid of these side-effects and focus on the chemically characteristic turnover parameters. Once the latter have been obtained, they can be used in the design of preparative-scale processes, taking into account, if necessary, transport factors and/or other side-phenomena that might occur in the preparative-scale conditions.

The catalytic reaction that we analyze here is depicted in Scheme 1. The catalyst couple P/Q is a reversible couple, characterized by a standard potential  $E_{P/Q}^0$ . We consider the case of a reduction, transposition to oxidation being straightforward. The catalytic reaction may involve several steps, but they are equivalent to an overall reaction with an apparent rate constant,  $k$ , in which the active form of the catalyst, Q, is used up to transform the substrate A and regenerate the initial form of the catalyst, P. Although the main features that we want to discuss could be delineated in the framework of such a one-electron process, we consider to be closer to common practice a second electron-transfer step in

Received: April 13, 2012

Published: June 6, 2012

## Scheme 1



which the intermediate B is rapidly consumed to give the final product C. In this two-electron process, shown on the left-hand side of Scheme 1, the second step is so fast that the Q+A reaction is rate-determining. Another possibility is shown on the right-hand side of Scheme 1, corresponding again to a global two-electron process in which the first one-electron reaction is rate-determining. The following analyses apply to one or the other of these reaction schemes and, more generally, to any two-electron process in which the first one-electron reaction is rate-determining. The one-electron reaction may itself consist of more than one step. Besides electrons, other reagents, e.g., acids, may interfere at this level. In this sense,  $k$  is a global rate constant that does not necessarily characterize a single rate-determining step.

In the framework of this general scheme, how can the TON and TOF be defined in conditions of preparative-scale electrolysis in systems where the catalyst stands in a film deposited on the electrode surface or a set of molecules dispersed in the solution? In all cases, we take into consideration only reactions that are fast enough to make the system irreversible (no reverse trace in, e.g., cyclic voltammetry), i.e., reactions that are sufficiently fast to be the basis of a worthwhile practical system. Throughout the paper we treat the case where the P/Q electron transfer is fast, so that the Nernst law will be applicable to the P/Q couple (the case of a slower electron transfer will be briefly discussed in the Concluding Remarks). The above reaction scheme corresponds to a first-order reaction in catalyst, as is most often encountered in practice. However, catalyst reaction order of 2 may sometimes occur, as discussed in, e.g., hydrogen evolution catalysis.<sup>12</sup> An extension to this case is described in the Supporting Information (SI), giving rise to the definition of experimental criteria allowing the discrimination between first-order and second-order situations.

The organization of the Discussion is as follows:

In the first section, we define and analyze the TON and TOF in conditions of preparative-scale electrolysis in the absence of side-phenomena. The first subsection is devoted to heterogeneous reactions, and the second to homogeneous reactions. We emphasize at this occasion that a fair and meaningful comparison between the two situations requires counting, in the latter case, only the catalyst present in the reaction layer, contrary to current practice that takes into account the catalyst present in whole cell compartment. The third subsection emphasizes the notion that TOF and overpotential ( $\eta$ ) are not independent parameters, but, contrary to frequent perception, there exists a precise relationship between the two factors. What is commonly shared in catalyst benchmarking is the obvious notion that a good catalyst is characterized by a high TOF and a small  $\eta$ , and vice versa. We develop another concept, namely that each particular catalyst is characterized by its own TOF- $\eta$  relationship. It is the comparison between the TOF- $\eta$  relationships that allows rational catalyst benchmarking. The characteristics of the TOF- $\eta$  relationships are

analyzed in detail, leading to the notion of intrinsic turnover frequency (TOF<sub>0</sub>, or turnover frequency at zero overpotential) as representing the intrinsic catalytic properties of the molecule under examination.

The second section is dedicated to foot-of-the-wave analysis of cyclic voltammetric data that allows a quick prediction of TOF<sub>0</sub> and its relationship with  $\eta$  as a help to select the most appropriate conditions for preparative-scale electrolysis. The efficiency of the method is illustrated in three perturbed situations created by the occurrence of substrate consumption, catalyst severe deactivation, or inhibition by product. Unperturbed responses are the object of the first subsection, whereas the above three side-phenomena are treated in the three subsequent subsections.

In the third section the application of the foot-of-the-wave approach is illustrated by examples taken from the homogeneous catalysis of CO<sub>2</sub> reduction by iron(0) porphyrins upon addition of Brønsted acids.

## DISCUSSION

### 1. Preparative-Scale Electrolysis. 1.1. Heterogeneous Reactions.

Figure 1 depicts the main features of the kinetic

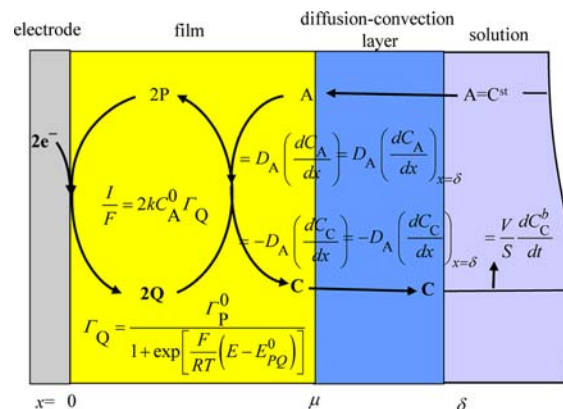


**Figure 1.** Catalysis and diffusion for a heterogeneous catalytic reaction under preparative-scale steady-state conditions. For symbols and equations, see text.

diffusion system for a heterogeneous catalytic reaction under preparative-scale steady-state conditions, where the catalyst is deposited on the electrode surface.  $x$  is the coordinate for diffusion, assumed as being linear,  $\mu$  is the thickness of the catalytic film, and  $\delta$  is the thickness of the diffusion-convection layer, depending on the rate of stirring of the solution or the circulation rate in flow cells.  $S$  is the electrode surface area,  $V$  the volume of the solution, and  $\Gamma_P$  and  $\Gamma_Q$  are the surface concentrations of the two forms of the catalyst, their total concentration being denoted  $\Gamma_P^0$ .  $C_A$  and  $C_C$  are the concentrations of the substrate and product, respectively;  $C_A^b$  and  $C_C^b$  are the concentrations of the substrate and product in the bulk, respectively.  $C_A^0$  is the initial concentration of substrate, and  $I$  is the current density ( $i$  is the current) flowing through the electrode. The equations figured in the various space zones of Figure 1 describe the way in which the catalytic current in the film triggers a flux of A toward the electrode and the production of a flux of C toward the solution (diffusion coefficients,  $D_A$ ), resulting in the consumption of A and production of C in the bulk of the solution.<sup>13,14</sup> The latter

concentration is thus obtained, from the combination of the various equations in Figure 1, as

$$\frac{dC_C^b}{dt} = -\frac{SD_A}{V} \left( \frac{dC_C}{dx} \right)_{x=\delta} = \frac{IS}{FV}$$

Since

$$\frac{I}{F} = \frac{2kC_A^0\Gamma_P^0}{1 + \exp\left[\frac{F}{RT}(E - E_{PQ}^0)\right]}$$

then

$$C_C^b = \frac{2kC_A^0\Gamma_P^0}{1 + \exp\left[\frac{F}{RT}(E - E_{PQ}^0)\right]} \frac{S}{V} t$$

The turnover number is defined as the number of moles of substrate transformed by 1 mol of both forms of the catalyst present on the surface,

$$\text{TON} = \frac{\text{mol C}}{\text{mol (P+Q)}} = \frac{C_C^b V}{\Gamma_P^0 S} = \frac{2kC_A^0 t}{1 + \exp\left[\frac{F}{RT}(E - E_{PQ}^0)\right]}$$

and the turnover frequency ( $s^{-1}$ ) is defined as

$$\text{TOF} = \frac{2kC_A^0}{1 + \exp\left[\frac{F}{RT}(E - E_{PQ}^0)\right]}$$

We do not consider in this discussion the notion of TON applied to unstable catalysts, sometimes defined as the number of catalytic cycles made by the catalyst before it has been completely deactivated. In such cases, our definitions would imply that the TOF decreases with time. We, of course, do not imply that analyzing the consequences of catalyst instability is not an important issue. A rational approach to this problem, however, requires as a preliminary an in-depth analysis of the stable catalyst case, such as the one we are attempting to produce in the present contribution.

In enzymatic catalysis, the TON and the TOF refer to maximum turnover in the framework of Michaelis–Menten kinetics, when  $C_A^0$  has reached a limiting maximal value. In the reactions we discuss here, the pseudo-first-order rate constant  $kC_A^0$  continues to increase with substrate concentration. In this sense it is not exactly the intrinsic parameter we are looking for. Second-order TON and TOF would be more appropriate for this purpose:

$$\text{TON}^{(2)} = \frac{2kt}{1 + \exp\left[\frac{F}{RT}(E - E_{PQ}^0)\right]} \quad (1)$$

$$\text{TOF}^{(2)} = \frac{2k}{1 + \exp\left[\frac{F}{RT}(E - E_{PQ}^0)\right]} \quad (2)$$

The TON and TOF are thus functions of the electrode potential,  $E$ , and therefore of the overpotential ( $\eta$ ), defined as the difference between the potential at which the electrode is operated and the standard potential for the formation of C from A,  $E_{AC}^0$ :  $\eta = E_{AC}^0 - E$ . This dependence will be discussed in more details in section 1.3.

**1.2. Homogeneous Reactions.** The situation is somewhat different in the case of a homogeneous catalytic reaction (Figure 2). The Q-concentration profile,  $C_Q(x)$  is restricted to a thin reaction–diffusion layer adjacent to the electrode surface.

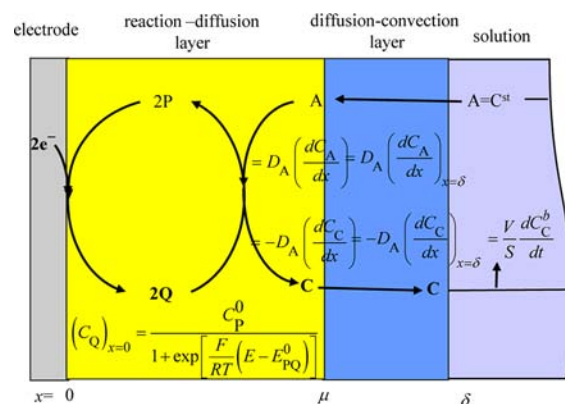


**Figure 2.** Catalysis and diffusion for a homogeneous catalytic reaction under preparative-scale steady-state conditions. For symbols and equations, see text.

(its thickness is of the order of  $\mu = (D_P/2kC_A^0)^{1/2}$ ,<sup>15</sup> where  $D_P$  is the diffusion coefficient of P and Q), within which

$$D_P \frac{d^2 C_Q}{dx^2} - 2kC_A^0 C_Q = 0,$$

with  $(C_Q)_{x=\mu} = 0$ ,  $\left( \frac{dC_Q}{dx} \right)_{x=\mu} = 0$

the concentration of Q at the surface obeying the Nernst law;  $C_P^0$  is the total concentration of catalyst.

The expression of the current density ensues:

$$\frac{I}{F} = \sqrt{2kC_A^0 D_P} \frac{C_P^0}{1 + \exp\left[\frac{F}{RT}(E - E_{PQ}^0)\right]} \quad (3)$$

Within the reaction–diffusion layer, the Q profile, obtained by space integration of the above differential equation and boundary conditions, may be expressed as

$$C_Q(x) = (C_Q)_{x=0} \exp\left(-\sqrt{\frac{2kC_A^0}{D_P}} x\right)$$

We consider the total amount of the catalyst, including both forms, per unit surface area in the reaction layer, by analogy to the definition we have used in the heterogeneous case, leading to

$$\text{mol (P+Q)}_\mu = S \sqrt{\frac{D_P}{2kC_A^0}} C_P^0$$

leading to exactly the same expressions of TON<sup>(2)</sup> (eq 1) and TOF<sup>(2)</sup> (eq 2) as in the heterogeneous case.

We thus see that a fair comparison of the performances of heterogeneous and homogeneous catalysts requires counting only the catalyst present in the reaction layer. This is at variance with frequent practice, which takes the catalyst present in the whole solution into account in the determination of the TON and TOF. This not only unduly disadvantages homogeneous catalysis toward heterogeneous catalysis but, even worse, does not reflect the actual properties of the catalyst, by introduction of a pointless cell volume-to-surface ratio. We note, *en passant*, that the catalyst present in the solution outside the reaction layer may serve as a useful stock in case the catalytic reaction is

accompanied by deactivation of the catalyst, thus increasing the lifetime of the system.

### 1.3. Turnover Frequency vs Overpotential Relationship.

Introducing the overpotential,  $\eta = E_{AC}^0 - E$ , eq 2 may be recast as

$$\text{TOF}^{(2)} = \frac{2k}{1 + \exp\left[\frac{F}{RT}(E_{AC}^0 - E_{PQ}^0 - \eta)\right]} \quad (4)$$

showing that there is a definite relationship between TOF and  $\eta$  that characterizes fully the catalytic properties of each molecule under examination.

As will be discussed later on, side-phenomena are minimized for low values of  $\eta$  and TOF. Under these conditions eq 4 may be simplified, leading to a Tafel-like expression relating TOF to  $\eta$ :

$$\log \text{TOF}^{(2)} = \log 2k - \frac{F}{RT \ln 10}(E_{AC}^0 - E_{PQ}^0) + \frac{F\eta}{RT \ln 10} \quad (5)$$

which provides a precise characterization of how good is the catalyst, opening the choice of operating catalysis with a low  $\eta$  and a low TOF or *vice versa*. An intrinsically good catalyst is thus a catalyst characterized by a large value of

$$\log \text{TOF}_0^{(2)} = \log 2k - \frac{F}{RT \ln 10}(E_{AC}^0 - E_{PQ}^0)$$

$\text{TOF}_0^{(2)}$  is what we may call the intrinsic turnover frequency of the catalyst (TOF at zero overpotential).

**2. Foot-of-the-Wave Analysis of Cyclic Voltammetric Responses.** We now address the possibility of a quick estimation of the TON and TOF from the cyclic voltammetry (CV) of the catalytic reaction, avoiding the burden of carrying out preparative-scale electrolyses for screening catalysts.

**2.1. Unperturbed Catalytic Responses.** If no side-phenomenon perturbs the catalytic reaction, the CV response is of the type shown in Figure 3a. Insofar as the reaction is fast as compared to  $Fv/RT$ , in which  $v$  is the scan rate, one obtains the classical S-shaped catalytic wave, independent of scan rate, of the following equation:<sup>16,3</sup>

$$\frac{i}{FS} = \frac{C_P^0 \sqrt{D_P} \sqrt{2kC_A^0}}{1 + \exp\left[\frac{F}{RT}(E - E_{PQ}^0)\right]}$$

The peak current of the catalyst in the absence of substrate,<sup>17</sup>

$$\frac{i_p^0}{FS} = 0.446 \times C_P^0 \sqrt{D_P} \sqrt{\frac{Fv}{RT}}$$

may serve to calibrate the catalytic response in terms of electrode surface area,  $S$ , catalyst concentration,  $C_P^0$ , diffusion coefficient,  $D_P$ , and scan rate,  $v$ . It is thus convenient to observe the variation of

$$\frac{i}{i_p^0} = \frac{2.24 \sqrt{\frac{RT}{Fv}} 2kC_A^0}{1 + \exp\left[\frac{F}{RT}(E - E_{PQ}^0)\right]}$$

Plotting  $i/i_p^0$  vs  $1/\{1 + \exp[(F)/(RT)(E - E_{PQ}^0)]\}$  thus gives rise to a straight line, the slope of which,  $2.24((RT/Fv))^{1/2}(2kC_A^0)^{1/2}$ , gives immediate access to  $2k$  and therefore to  $\text{TOF}^{(2)}$ , and to the  $\text{TOF}_0^{(2)}-\eta$  relationship (eq 4 or 5) as

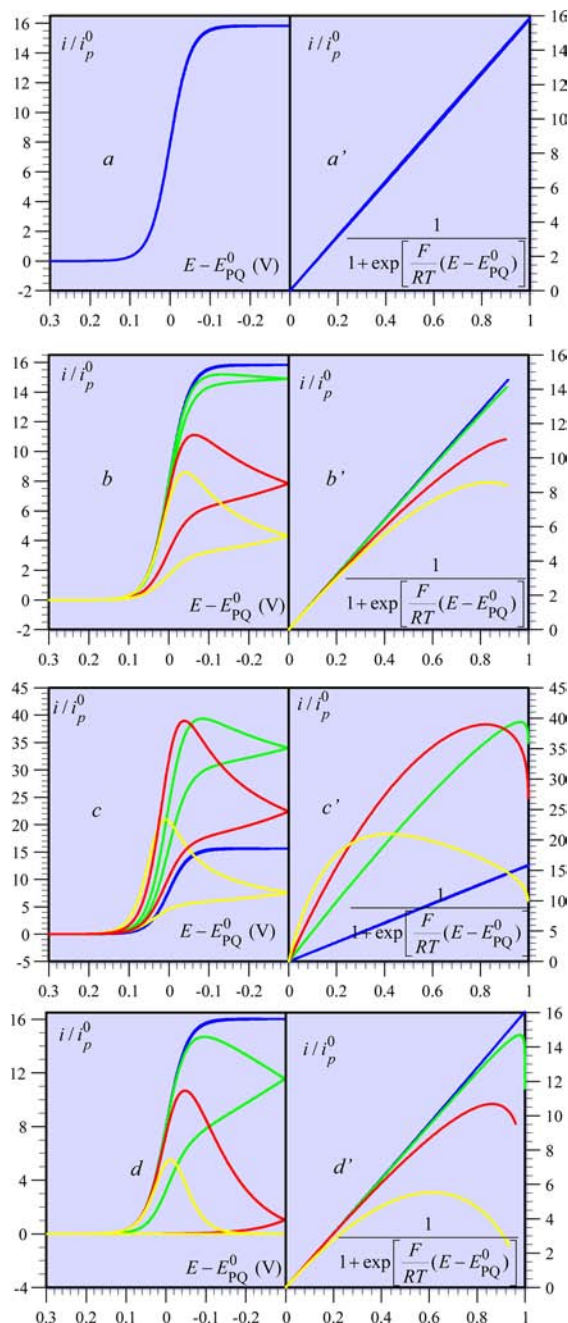


**Figure 3.** Catalytic CV responses (left) and foot-of-the-wave analyses (right) for a typical system,  $v = 0.1$  V/s,  $D_P = 10^{-5}$  cm<sup>2</sup> s<sup>-1</sup>,  $C_P^0 = 1$  mM,  $T = 298$  K. (a,a')  $C_A^0 = 1$  M,  $2k = 100$  M<sup>-1</sup> s<sup>-1</sup>, no side-phenomenon. (b,b') Substrate consumption. From blue to yellow:  $C_A^0 = 1, 0.1, 0.01$ , and  $0.005$  M;  $2kC_A^0 = 100$  s<sup>-1</sup>. (c,c') Deactivation of the catalyst by a co-catalyst (Scheme 2).  $C_A^0 = 1$  M,  $2k = 100$  M<sup>-2</sup> s<sup>-1</sup>;  $k' = 10^{10}$  M<sup>-1</sup> s<sup>-1</sup>;  $k_{deact} = 10^7$  M<sup>-2</sup> s<sup>-1</sup>. From blue to yellow:  $k_{deact}[Z]/(k' + k_{deact}[Z]) = 0, 0.01, 0.03, 0.1$ . (d,d') Inhibition by the product of the reaction (Scheme 3).  $C_A^0 = 1$  M,  $2k = 100$  M<sup>-1</sup> s<sup>-1</sup>. Surface concentration of the adsorbed product when electrode surface is totally blocked:  $\Gamma^0 = 5.75 \times 10^{-9}$  mol cm<sup>-2</sup>. From blue to yellow:  $\log k_a = -8.4, -6.4, -5.4$ , and  $-4.4$  cm s<sup>-1</sup>.

illustrated in Figure 3a,a', with typical values of the various parameters.

There are several possible side-phenomena that may perturb such a simple catalytic response, as discussed in the next subsections.

**2.2. Consumption of the Substrate.** In the first row of these side-phenomena is the consumption of the substrate, A. Figure 3b gives a typical example of such a situation, in which the decrease of the substrate concentration results in an increasing contribution of its diffusion toward the electrode in the CV responses, which deviates more and more from the S-shaped classical response. Application of the above foot-of-the-wave analysis (Figure 3b') allows the observation of a straight line at the foot of the wave, devoid of distortion resulting from the interference of substrate consumption. As the consumption of the catalyst becomes more and more significant, the potential range where the foot-of-the-wave analysis applies narrows so much as to render the method ineffective. In such a "total catalysis" situation, where the system is governed by substrate diffusion, the catalytic rate constant may simply be derived from the peak potential.<sup>13,16b</sup>

**2.3. Deactivation of the Catalyst.** A second possibility is the deactivation of the catalyst. Beyond the simplest one,<sup>18</sup> we consider here a case where deactivation is more severe as the co-catalyst, Z, is also responsible for catalyst deactivation (Scheme 2), as suspected in recent investigations of the homogeneous catalysis of CO<sub>2</sub> reduction by iron(0) porphyrins, where Z represents Brönsted acids,<sup>19</sup> and catalyst deactivator (eq 1).

Scheme 2

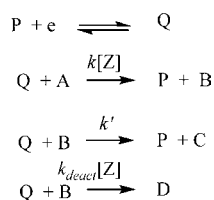
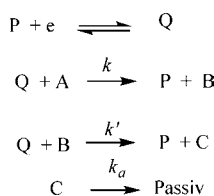


Figure 3c shows how an increase in the concentration of the co-catalyst and co-deactivator, Z, makes the CV response deviate more and more from the S-shaped behavior. Figure 3c' illustrates how the application of the foot-of-the-wave analysis allows one to get rid of the effect of catalyst deactivation, leading to TOF<sub>0</sub><sup>(2)</sup> and to the TOF<sub>0</sub><sup>(2)</sup>- $\eta$  relationship (eqs 4 and 5).

**2.4. Inhibition by Product.** The third perturbation we consider is caused by inhibition of the current by the product of the reaction according to Scheme 3. Adsorption of the product

Scheme 3



C is assumed to obey the Langmuir isotherm and to totally block the portion of the surface where it takes place. Under these conditions, the current is given by

$$\frac{i}{FS} = (1 - \theta) \frac{C_P^0 \sqrt{D_P} \sqrt{2kC_A^0}}{1 + \exp\left[\frac{F}{RT}(E - E_{PQ}^0)\right]}$$

The fraction,  $\theta$ , of the electrode surface inactivated by product adsorption is a function of the rate constant of adsorption,  $k_a$ , besides other parameters. The theory and simulation procedures for such systems have been described in detail.<sup>20</sup> Application to the present illustrating example (Figure 3d) shows the distorting effect of an acceleration of the inhibiting adsorption. Here too, application of the foot-of-the-wave analysis allows one to obviate the effect of the side-phenomenon and derive the TOF<sub>0</sub><sup>(2)</sup> and the TOF<sub>0</sub><sup>(2)</sup>- $\eta$  relationship (eqs 4 and 5).

**3. Application to the Catalysis by Fe<sup>0</sup> Tetraphenylporphyrin in the Presence of Phenol.** **3.1. Foot-of-the-Wave Analysis of Cyclic Voltammetric Responses.** Although the foot-of-the-wave approach is a general methodology, a practical test of its applicability would seem appropriate. We selected as such an illustrative example the reduction of CO<sub>2</sub> into CO catalyzed by Fe<sup>0</sup> tetraphenylporphyrin (FeTPP) in dimethylformamide (DMF) in the presence of phenol ( $E_{PQ}^0 = -1.428$  V vs SHE). The results obtained at 0.1 V/s and at a CO<sub>2</sub> concentration of 0.23 M, with three PhOH concentrations, 0.1, 0.75, and 3 M are displayed in Figure 4. Without going into the details of the reaction mechanism, the reaction scheme is of the type represented on the left of Scheme 1, as depicted in Scheme 4.

The rate-determining reaction, with the overall rate constant  $k$ , may consist of several steps. The reaction order in PhOH is therefore not necessarily 2, as indicated in the global reaction. One thrust of the mechanistic analysis is precisely to determine this reaction order.

As seen in Figure 4, which gathers several experiments done at 0.1 V/s, the normalized cyclic voltammograms differ from the standard S-shaped response in the sense that the increase in current is accompanied by the appearance of a peak rather than of a plateau. The peak shape is more and more pronounced as [PhOH] is raised. Another manifestation of the same phenomenon can be observed in Figure 4, where it is shown that deviation from linearity of the foot-of-the-wave analysis increases with [PhOH]. These deviations are caused by the increase of the rate constant with [PhOH], which results in a rise of the charge flowing through the electrode surface, thus triggering a growing interference of the side-phenomena discussed earlier. Restricting the foot-of-the-wave to its linear portion allows the determination of the rate constant in all cases:<sup>21</sup>  $2k = 1.6 \times 10^4$ ,  $1.3 \times 10^5$ , and  $9 \times 10^5$  M<sup>-1</sup> s<sup>-1</sup> for [PhOH] = 0.1, 0.75, and 3 M, respectively, in line with the participation of phenol in the catalytic reaction.

Raising the scan rate is a means of enlarging toward negative potentials the domain in which the voltammogram and the foot-of-the-wave analysis adhere to the standard behavior, as expected from the fact that the charge flowing through the electrode surface decreases accordingly and so for the interference of the side-phenomena. These predictions are tested successfully as shown in Figure 5 for [PhOH] = 3 M, where the maximal deviation was observed (Figure 4), leading to a better precision on the determination of  $k$  for this phenol concentration.

**3.2. Predicted Turnover Frequency vs Overpotential Relationship.** The potential-dependent values of the TOF that can be derived from these "foot-of-the-wave" analyses may now be recast under the form of a TOF- $\eta$  relationship (eqs 4 and 5), after the standard potential for the global reaction taking place during catalysis,  $E_{\text{CO}_2/\text{CO,DMF}}^0$ , has been estimated.

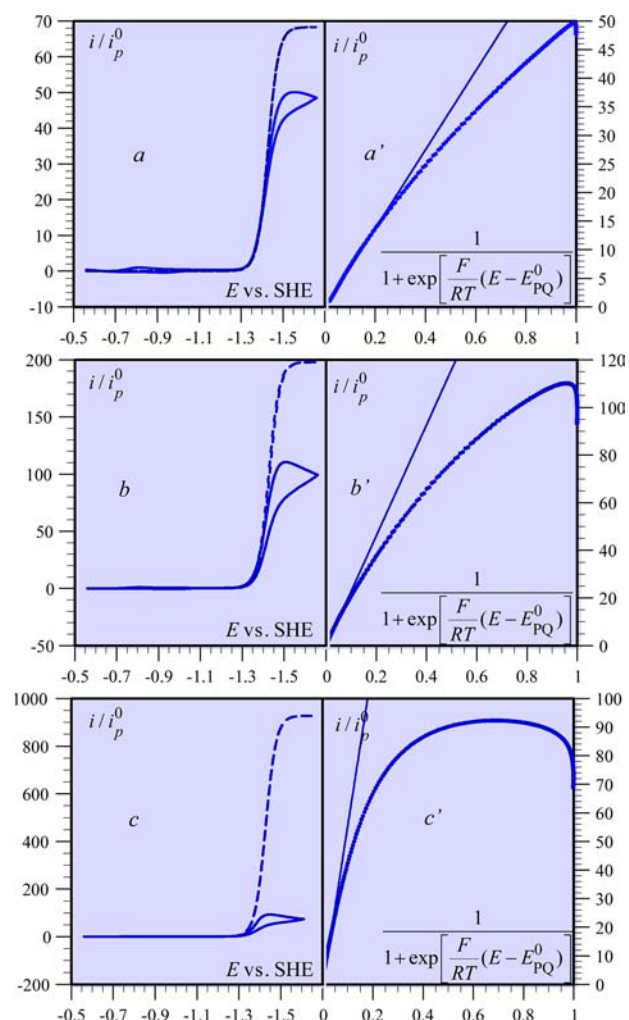
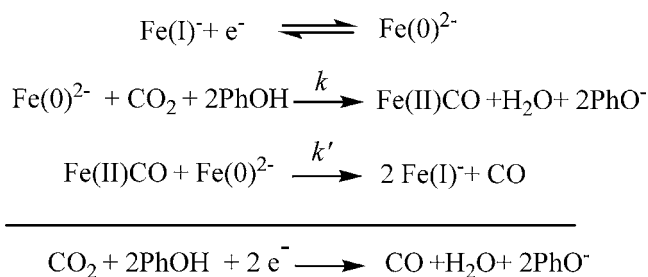
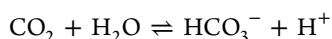


**Figure 4.** Cyclic voltammety of Fe(TPP) (1 mM) in DMF + 0.1 M  $n$ -Bu<sub>4</sub>NPF<sub>6</sub> in the presence of 0.23 M CO<sub>2</sub> and 0.1 (a,a'), 0.75 (b,b'), and 3 (c,c') M PhOH (left and right, respectively) on a Hg electrode at 21 °C and a scan rate 0.1 V/s. (a,b,c) CV responses: solid line, experiments; dashed line, simulation of the corresponding hypothetical unperturbed catalytic responses. (a',b',c') Foot-of-the-wave analyses.

#### Scheme 4



The overall reaction in Scheme 4 indicates that  $E_{\text{CO}_2/\text{CO,DMF,PhOH}}^0$  should depend upon the pK of the acid present, here phenol. In fact there is a stronger acid in the DMF medium, namely, CO<sub>2</sub> itself in the presence of residual water:



The proper reaction to be considered is therefore

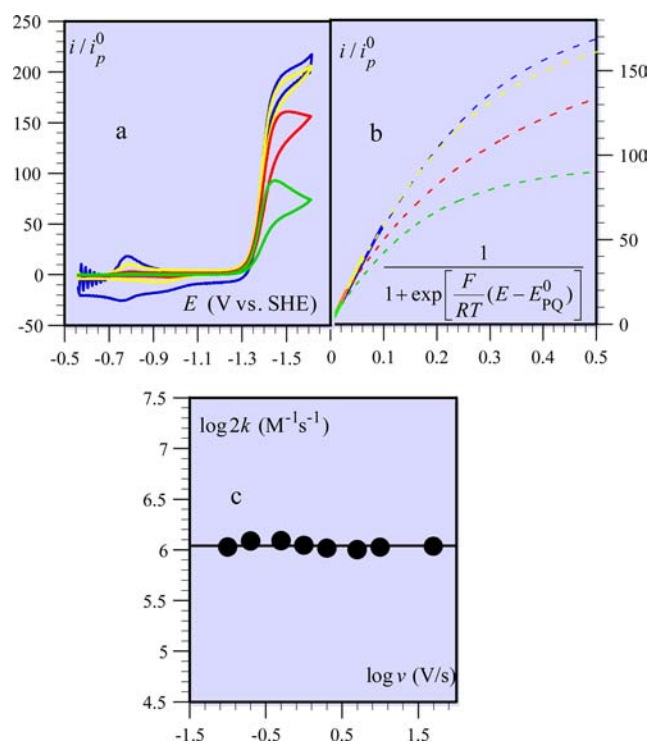
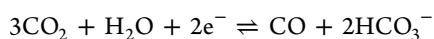


**Figure 5.** Cyclic voltammety of 1 mM Fe(TPP) in DMF + 0.1 M  $n$ -Bu<sub>4</sub>NPF<sub>6</sub> in the presence of 0.23 M CO<sub>2</sub> and 3 M PhOH on a Hg electrode at 21 °C. Variations with the scan rate: 0.1 (green), 1 (red), 10 (yellow), and 50 V/s (blue). (a) CV responses and (b) foot-of-the-wave analyses. The dashed curves are the raw analyses; the solid curves their linear portions. (c) Rate constant from the slopes of the linear portions in b, derived at more scan rates than shown in b.

leading to  $E_{\text{CO}_2/\text{CO,DMF}}^0 = -0.694$  V vs SHE (see SI). The TOF- $\eta$  relationships lead to the representation in Figure 6.

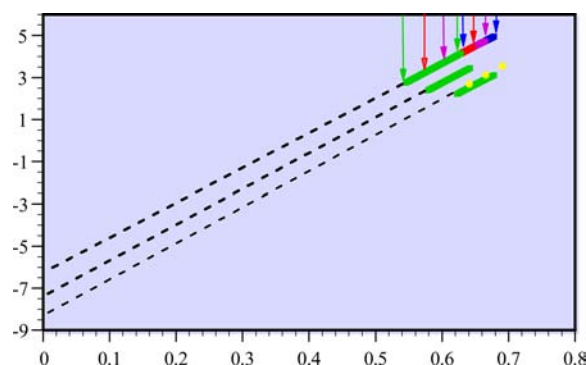


**Figure 6.** TOF<sup>(2)</sup> vs  $\eta$  Tafel lines for, from bottom to top, 0.1, 0.75, and 3 M PhOH. The green segments are derived from 0.1 V/s experiments. The red, magenta, and blue segments shown for [PhOH] = 3 M, were obtained at 1, 10, and 50 V/s, respectively. The colored arrows indicate the length of the  $\eta$  interval browsed at each scan rate. The yellow dots represent the electrolyses at -1.335, -1.36, and -1.385 V vs SHE (see text and Figure 7 below).

The corresponding intrinsic turnover frequencies ensue as measures of the intrinsic properties of the catalyst + phenol system: TOF<sub>0</sub><sup>(2)</sup> =  $6.2 \times 10^{-8}$ ,  $4.9 \times 10^{-9}$ , and  $3.5 \times 10^{-7}$  for [PhOH] = 0.1, 0.75, and 3 M, respectively.

**3.3. Preparative-Scale Electrolysis.** Preparative-scale electrolyses were run on a 20 cm<sup>2</sup> mercury pool cathode in a cell

described in the SI. Particular care was exerted to minimize the ohmic drop by positioning the reference electrode close to the cathode (see SI). In a first experiment, the electrode potential was scanned slowly (10 mV/s) to let the steady-state conditions unperturbed. The results are shown in Figure 7.

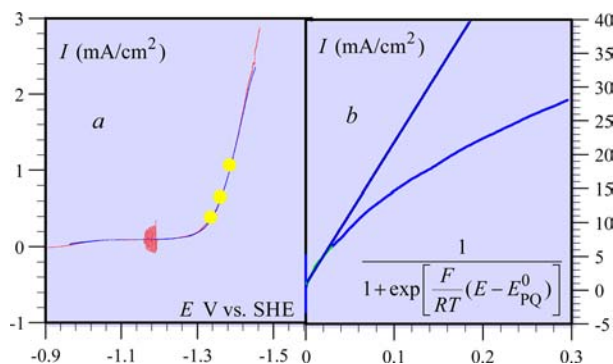


**Figure 7.** Electrolyses of a DMF + 0.1 M *n*-Bu<sub>4</sub>NPF<sub>6</sub> solution of FeTPP (1 mM), in the presence of 0.23 M CO<sub>2</sub> and 0.1 M PhOH on a 19.6 cm<sup>2</sup> mercury pool electrode. (a) Current density vs potential curves obtained with a slow potential scan (10 mV/s); red and blue curves correspond to two successive experiments. Yellow dots: 5 min electrolysis at -1.335, -1.36, and -1.385 V vs SHE. (b) Foot-of-the-wave analyses.

The steady state is in fact the result of a steady-state catalytic response (see section 1.2) rather than of a steady-state transport.<sup>22</sup> In an additional series of experiments, the potential was fixed and a few (3–5) minutes of electrolysis was performed, giving rise to stable currents, the representative points of which stand, as expected, on the slow scan curves (Figure 7a).

An analysis similar to the foot-of-the-wave analysis in CV is obtained by application of eq 3. It allows the determination (Figure 7b) of the interval of electrode potential where catalysis is not perturbed by side-phenomena. The latter effects may indeed decrease the catalytic current similarly to what has been seen in CV. The values of the rate constant,  $2k = 1.7 \times 10^4 \text{ M}^{-1} \text{ s}^{-1}$  and  $\text{TOF}_0^{(2)} = 1.6 \times 10^{-6} \text{ M}^{-1} \text{ s}^{-1}$ , are in good agreement with the values derived from the foot-of-the-wave analysis in CV ( $2k = 1.6 \times 10^4 \text{ M}^{-1} \text{ s}^{-1}$ ,  $\text{TOF}_0^{(2)} = 1.5 \times 10^{-6} \text{ M}^{-1} \text{ s}^{-1}$ ) for the same concentration of PhOH. Equivalently, it is seen in Figure 6 that the yellow dots representing the three electrolyses stand with a good accuracy on the  $\log \text{TOF}^{(2)} - \eta$  line derived from the foot-of-the-wave analysis of the CV responses.

More prolonged electrolyses were performed in order to quantitate the product formation. For example, a 1-h electrolysis at -1.46 V vs SHE in the presence of 0.1 M PhOH produces  $1.68 \times 10^{-4} \text{ mol}$  of CO after the passage of 35 C, i.e., a faradaic yield of 92.5%. This corresponds to 6 million cycles achieved by the catalyst molecules in the reaction–diffusion layer without degradation. More preparative-scale results obtained in the presence of several acids at various concentrations will be given elsewhere. We restricted ourselves here to the demonstration of the validity of the methodology we propose.

## CONCLUDING REMARKS

The first step of our discussion was a clarification of the notion of turnover number and turnover frequency of catalyzed electrochemical reactions that would characterize the catalyst

chemically regardless of side-phenomena such as mass transport, product inhibition, and catalyst deactivation. It was then shown that a catalyst is not chemically characterized by its TOF and/or its overpotential but that, in fact, TOF and  $\eta$  are functions of one another. This relationship often takes the form of a Tafel law, allowing the definition of a characteristic turnover frequency,  $\text{TOF}_0$  (the TOF at zero overpotential). Comparison of  $\text{TOF}_0$  values allows one to delineate intrinsically good and bad catalysts.

The foot-of-the-wave analysis of the cyclic voltammetric catalytic responses allows determination of the TOF, the TOF vs  $\eta$  relationship, and the  $\text{TOF}_0$  independently of the side-phenomena that interfere at high current densities and prevent the expected current plateau from being reached. The validity of this methodology has been established on theoretical grounds and checked experimentally with examples taken from an ongoing systematic study of the catalytic reduction of CO<sub>2</sub> by iron(0) porphyrins in the presence of Brønsted acids.

For the sake of simplicity and because it is often relevant, we have treated only the case where the catalyst redox couple is fast, so fast as to obey the Nernst law. Adaptation to the case of slower electron transfer is straightforward, provided the P/Q standard rate constant,  $k_s$ , and the transfer coefficient,  $\alpha$  (generally close to 0.5), are known, replacing eq 3 by

$$\frac{I}{F} = \frac{\sqrt{2kC_A^0 D_P C_P^0}}{1 + \exp\left[\frac{F}{RT}(E - E_{PQ}^0)\right] + \frac{\sqrt{2kC_A^0 D_P}}{k_s} \exp\left[\frac{\alpha F}{RT}(E - E_{PQ}^0)\right]}$$

In the illustrating example we have analyzed, as in most practical situations, side-phenomena are so prevalent that control of the catalytic reaction by the intrinsic properties of the catalyst requires relatively low current densities. This is true both in CV catalyst screening and in preparative-scale electrolysis. In the latter case, higher current densities may well be required for getting practically satisfying TOFs. It should simply be borne in mind that several other factors, not always easy to identify, are thus likely to interfere besides the intrinsic properties of the catalyst. In these conditions, comparison between catalysts may well become meaningless. Just to take one example: in cases where ohmic drop is an important current-limiting factor, comparison between catalysts may well turn out to actually be comparison between cell designs. These observations emphasize the interest of a preliminary foot-of-the-wave analysis of CV catalytic responses. A rapid answer, rid of side-phenomena, is easily obtained, which can then be taken as the basis for devising an appropriate preparative-scale strategy.

## ASSOCIATED CONTENT

### Supporting Information

Experimental details; determination of  $E_{\text{CO}_2/\text{CO,DMF}}^0$  and the *meso*-tetraphenylporphyrin iron(III) diffusion coefficient. This material is available free of charge via the Internet at <http://pubs.acs.org>.

## AUTHOR INFORMATION

### Corresponding Author

saveant@univ-paris-diderot.fr

## Notes

The authors declare no competing financial interest.

## ACKNOWLEDGMENTS

Partial financial support from the Agence Nationale de la Recherche (ANR 2010 BLAN 0808) is gratefully acknowledged.

## REFERENCES

- (1) Lewis, N. S.; Nocera, D. G. *Proc. Natl. Acad. Sci. U.S.A.* **2006**, *103*, 15729.
- (2) Felton, G. A. N.; Glass, R. S.; Lichtenberger, D. L.; Evans, D. H. *Inorg. Chem.* **2006**, *45*, 9181.
- (3) Savéant, J.-M. *Chem. Rev.* **2008**, *108*, 2348.
- (4) Benson, E. E.; Kubiak, C. P.; Sathrum, A. J.; Smieja, J. M. *Chem. Soc. Rev.* **2009**, *38*, 89.
- (5) Concepcion, J. J.; Jurss, J. W.; Brennaman, M. K.; Hoertz, P. G.; Patrocino, A. O. T.; Murakami Iha, N. Y.; Templeton, J. L.; Meyer, T. *J. Acc. Chem. Res.* **2009**, *42*, 1954.
- (6) DuBois, R. M.; DuBois, D. L. *Acc. Chem. Res.* **2009**, *42*, 1974.
- (7) Gloaguen, F.; Rauchfuss, T. B. *Chem. Soc. Rev.* **2009**, *38*, 100.
- (8) Artero, V.; Chavarot-Kerlidou, M.; Fontecave, M. *Angew. Chem., Int. Ed.* **2011**, *50*, 7238.
- (9) Bourrez, M.; Molton, F.; Chardon-Noblat, S.; Deronzier, A. *Angew. Chem., Int. Ed.* **2011**, *50*, 9903.
- (10) Du, P.; Eisenberg, R. *Energy Environ. Sci.* **2012**, *5*, 6012.
- (11) In CV or related techniques, about one-millionth of the substrate is consumed during each run, making these techniques “non-destructive” as opposed to bulk electrolyses.
- (12) (a) Hu, X.; Brunshwig, B. S.; Peters, J. C. *J. Am. Chem. Soc.* **2007**, *129*, 8988. (b) McCrory, C. C. L.; Uyeda, C.; Peters, J. C. *J. Am. Chem. Soc.* **2012**, *134*, 3164.
- (13) Savéant, J.-M. *Elements of Molecular and Biomolecular Electrochemistry*; Wiley-Interscience: New York, 2006; Chap. 2, pp 132–136.
- (14) We consider the case where the bulk substrate concentration remains constant throughout the experiment, e.g., the case when the substrate is the solvent (oxidation or reduction of water) or when it is constantly replenished, as in reduction of a gas maintained at constant pressure ( $O_2$ ,  $CO_2$ ).
- (15) Reference 13, p 82.
- (16) (a) Savéant, J.-M.; Vianello, E. In *Advances in Polarography*; Longmuir, I. S., Ed.; Pergamon Press: London, 1960; pp 367–374. (b) Savéant, J.-M.; Su, K. B. *J. Electroanal. Chem.* **1984**, *171*, 341. (c) Savéant, J.-M.; Vianello, E. *Electrochim. Acta* **1965**, *10*, 905. (d) Reference 13, pp 108–119.
- (17) Reference 13, p 7.
- (18) Reference 13, pp 115, 409, and 410.
- (19) Bhugun, I.; Lexa, D.; Saveant, J. M. *J. Am. Chem. Soc.* **1996**, *118*, 1769.
- (20) Bhugun, I.; Savéant, J.-M. *J. Electroanal. Chem.* **1996**, *408*, 5.
- (21) The potential range of applicability of the method was limited at its left-hand side by starting the analysis when  $i/i_p^0 > 1$ .
- (22) (a) The current oscillations that appear in front of the catalytic current rise in Figure 7a, indicating that the resistance between the working and reference electrodes, which is not compensated by the potentiostat, is minimized<sup>22b</sup> (see SI). (b) Reference 13, Chap. 1, pp 14–20; Chap. 6, pp 353–361.